FTIR spectroscopy as an analytical tool to compare glycosylation in therapeutic monoclonal antibodies

Allison Derenne[1], Kheiro-Mouna Derfoufi[1], Ben Cowper[2], Cédric Delporte[3] and Erik Goormaghtigh[1]

(1) Center for Structural Biology and Bioinformatics, Laboratory for the Structure and Function of Biological Membranes, Campus Plaine CP206/02; Université Libre de Bruxelles, Bld du Triomphe 2, CP206/2, B1050 Brussels, Belgium

(2) National Institute for Biological standards and Control, Blanche Lane, South Mimms, Potters Bar, Hertfordshire, EN6 3QG, United Kingdom

(3) RD3 - Pharmacognosy, Bioanalysis & Drug Discovery Unit & Analytical Platform of the Faculty of Pharmacy, Campus Plaine, CP2025/5, Université Libre de Bruxelles, Bld du Triomphe 2, CP205/5, B1050 Brussels, Belgium

Correspondence to:

Dr. Erik Goormaghtigh.

Center for Structural Biology and Bioinformatics, Laboratory for the Structure and Function of Biological Membranes, Campus Plaine CP206/02; Université Libre de Bruxelles, Bld du Triomphe 2, CP206/2, B1050 Brussels, Belgium

Tel.: +32-2-650-53-86; Fax: +32-2-650-53-82; E-mail: egoor@ulb.ac.be

1. Abstract

Glycosylation is the most common protein post-translational modification (PTM), especially in biopharmaceuticals. It is a critical quality attribute as it impacts product solubility, stability, half-life, pharmacokinetics and pharmacodynamics (PK/PD), bioactivity and safety (e.g. immunogenicity). Yet, current glycan analysis methods involve multiple and lengthy sample preparation steps which can affect the robustness of the analyses. The development of orthogonal, direct and simple method is therefore desirable. In this study, we suggest use of FTIR spectroscopy to address this challenge. Use of this technique, combined with statistical tools, to compare samples or batches in terms of glycosylation or monosaccharide profile, has three potential applications: to compare glycosylation of a biosimilar and the original (innovator) molecule, for monitoring of batch-to-batch consistency, and for in-process control. Fourteen therapeutic monoclonal antibodies (mAbs), one Fc-fusion protein and several other common glycoproteins have been used to demonstrate that FTIR spectra of glycoproteins display spectral variations according to their glycan and monosaccharide compositions. We show that FTIR spectra of glycoproteins provide a global but accurate fingerprint of the glycosylation profile. This fingerprint is not only sensitive to large differences such as the presence or absence of several monosaccharides but also to smaller modifications of the glycan and monosaccharide content.

2. Abbreviations

PTM, post-translational modification; FTIR, Fourier Transform Infrared; mAbs, monoclonal antibodies; RFMS, RapiFluor-Mass Spectroscopy; ATR, Attenuated total reflection; DMF, dimethylformamide; ACN, acetonitrile; HILIC, Hydrophilic interaction liquid chromatography; SPE, solid phase extraction; PCA, principal component analysis; PC, principal component; MANOVA, multivariate analysis of variance; GlcNac, *N*-acetylglucosamine; NANA/Neu5Ac, N-acetylneuraminic acid, NGNA/Neu5Gc, N-glycolylneuraminic acid, % RPA, relative peak area.

3. Keywords

FTIR spectroscopy; infrared; glycosylation; monoclonal antibodies; glycoproteins, biosimilar.

4. Introduction

Glycosylation is the most common protein post-translational modification (PTM), occurring in more than 60 % of biopharmaceuticals (monoclonal antibodies (mAbs), hormones, fusion proteins). It is defined as the attachment of glycans at specific sites within the amino acid chain of proteins. Obtaining an appropriate glycosylation profile is critical for product solubility, stability, half-life, pharmacokinetics and pharmacodynamics (PK/PD), bioactivity and safety (e.g. immunogenicity) [1–3]. Furthermore, protein glycosylation is influenced by many parameters during the manufacturing process. Each host system (mammalian cells, yeast strains, plant cells, insect cells or genetically modified animals) has its own glycosylation machinery which strongly affects the glycosylation profile. Specific non-human patterns, such as *N*-glycolylneuraminic acid (Neu5Gc), terminal α1-3 galactose-galactose (α-Gal-Gal), and α1-3 linked fucose, are reported to be immunogenic and may be more or less present according to the host type [3,4]. Additionally, it has also been shown that the cell culture environmental conditions (bioreactor type, culture media and process parameters) have a significant effect on the protein glycosylation profile [1,4,5].

Considering the variability that may occur in the glycosylation pattern and its impact on the quality and safety of the final therapeutic product, monitoring of the glycosylation profile – a critical quality attribute (CQA) – should be performed from clone selection and at each stage of the development process [1,6]. Regulatory agencies worldwide thus require robust, information-rich, reproducible and preferably orthogonal methods for glycosylation analysis at all stages of the development process to ensure accuracy and consistency of the final drug product [6].

However, glycosylation analysis has traditionally been a time-consuming process with long sample preparation protocols and manual data interpretation [7]. To address these challenges, we suggest the

use of FTIR spectroscopy as a convenient and powerful tool to compare protein samples and batches in terms of glycan and monosaccharide content. More precisely, we wish to address whether FTIR spectroscopy is able to provide unique signatures reflecting given glycosylation profiles and whether these signatures can be used to distinguish a series of antibodies with a similar (but not identical) glycan composition. This would pave the way to compare accurately the glycan profile of several batches or between biosimilars and innovators.

FTIR spectroscopy has already been widely used to analyse protein structure. These analyses are mainly based on the region of the FTIR spectrum between 1700 and 1500 cm^{-1}. This region contains the amide I and II bands resulting from the absorption of the carbonyl amide present in the peptide bond. A previous study by Zheng et al. has notably shown that the presence of specific glycoforms such as high-mannose or afucosylated structures does not alter the secondary structure of a mAb [8]. It is also established that carbohydrates associated with glycoproteins are responsible for absorption in other areas of the FTIR spectrum of these proteins. The most interesting area for studying saccharides is found between 1200 and 950 cm^{-1}. The contribution of glycosylation to the FTIR spectra of proteins has been addressed previously by Khajehpour et al. who recorded the spectra of five glycoproteins (and one protein without glycosylation) and analysed the region between 1200 and 1000 cm^{-1}. The glycosylation profiles of these proteins are very different as they contain specific distinct monosaccharides. This study showed that the intensity of these spectral bands was related to the amount of carbohydrates contained in the glycoprotein, and also noted that the shape of these bands varies with the type of monosaccharide present in the protein [9].

In this study, we have used FTIR and conventional *N*-glycan analysis method to characterize in detail the N-glycosylation profiles of 14 therapeutic mAbs, one Fc-fusion protein, and a further three glycoproteins:

- alpha1-acid glycoprotein which contains 5 *N*-glycan sites and a very high sialic acid content [10,11];

- ribonuclease B which contains high-mannose glycans [11,12];

- avidin which contains predominantly high-mannose glycans [11,13].

Fetuin, a well-characterized glycoprotein containing *O*- and *N*-glycans and with a high content of sialic acid [11,14,15] has also been analysed by FTIR only, since it contains a majority of *O*-glycans and therefore *N*-glycan analysis would not provide sufficient information for correlation with FTIR data.

Each antibody has a unique *N*-glycan profile, although compared to the four other glycoproteins, the glycosylation profiles of all mAbs are relatively similar. FTIR spectra of all glycoproteins have been recorded, and statistical tools used to compare spectra. The aim of the analysis is twofold:

1. To evidence large spectral variations between the mAbs and all other glycoproteins;
2. To demonstrate that smaller but significant variations are present among the FTIR spectra of the different mAbs.

5. Materials and methods

5.1. Chemical, reagents and proteins

Fourteen therapeutic mAbs and one therapeutic Fc-fusion protein have been obtained from the hospital Saint-Pierre (Brussels):

- Adalimumab (Humira 40 mg, Abbvie)
- Aflibercept (Zaltrap 100 mg 4 mL^{-1}, Sanofi-Aventis)
- Bevacizumab (Avastin 400 mg 16 mL^{-1}, Roche Pharma)
- Cetuximab (Erbitux, 500 mg 100 mL^{-1}, Merck KGaA)
- Infliximab (Remicade-100 mg, Janssen Biologics)
- Natalizumab (Tysabri-300 mg, Biogen)
- Nivolumab (Opdivo-40mg 4 mL^{-1}, Bristol Myer Squibb)
- Omalizumab (Xolair-75 mg 0.5 mL^{-1}, Novartis)
- Panitumumab (Vectibix-400 mg 20 mL^{-1}, Amgen)
- Pembrolizumab (Keytruda-50 mg, Merck)
- Pertuzumab (Perjeta-420mg 14 mL^{-1}, Roche Pharma)
- Ramucirumab (Cyramza-10mg mL^{-1}, Eli-Lilly)
- Rituximab (Mabthera-500 mg 50 mL^{-1}, Roche Pharma)
- Trastuzumab (Herceptin-150 mg, Roche Pharma)
- Trastuzumab-emtasine (Kadycla-160 mg, Roche Pharma)

Final formulations of therapeutic proteins generally contain excipients that may interfere with the FTIR measurements, especially in the spectral region between 1200 and 950 cm^{-1} which is specific to glycosylation. Therefore, a buffer exchange step was applied using Micro-Biospin™ P-6 Gel Columns (Bio-Rad #7326221, Tris buffer, sample volume 10-75 µL, 6000 daltons MW limit). The buffer was replaced by 0.9% NaCl. No dilution was performed before FTIR measurements.

Fetuin (F2379-100 mg), alpha1-acid glycoprotein (G9885-10 mg), ribonuclease B (R7884-100 mg), egg white avidin (A9275-10 mg) and sialic acid (A0812-100 mg) were purchased from Sigma-

Aldrich. Proteins were dissolved in 0.9% NaCl at 10 mg mL^{-1}. Residual salts or excipients were removed by using Micro-Biospin™ P-6 Gel Columns (Bio-Rad #7326221, Tris buffer, sample volume 10-75 µL, 6000 daltons MW limit) and replaced with 0.9% NaCl.

5.2. LC-FLR-MS N-glycans characterization

The *N*-glycans of the mAbs, aflibercept, alpha1-acid glycoprotein, ribonuclease B and egg white avidin were characterized using the Waters GlycoWorks RapiFluor-MS *N*-glycan 24 samples kit (#176003713). This recent approach both decreases the time required for sample preparation and enhances the sensitivity of *N*-glycan detection. [16]

5.2.1. Deglycosylation of glycoproteins

All protein samples (2 mg mL^{-1}) were diluted to a concentration of 0.52 mg mL^{-1} by addition of 7.5 µL volume to 6 µL of 5% (w/v) RG surfactant (RapiGest SF, Waters, Milford, MA) and 15.3 µL water. Samples were heated to 95 °C for 2 min, allowed to cool to 50 °C, before the addtition of 1.2 µL of PNGase F solution (GlycoWorks Rapid PNGase F, Waters, Milford, MA). Deglycosylation was completed by incubating the samples at 50 °C for 5 min [7,16].

5.2.2. Glycan labelling

Samples from PNGase F digestion were allowed to cool to room temperature before addition of 12 µL of 127 mM RFMS, dissolved in anhydrous dimethylformamide (DMF) (RapiFluor-MS, Waters, Milford, MA) without a protein depletion step. Labelling reactions were allowed to proceed at room temperature for 5 min. The reaction was then quenched with addition of 358 µL of acetonitrile (ACN), which also adjusted the solution to an appropriate organic solvent concentration for HILIC-based purification [7,16].

5.2.3. Glycan purification

The ACN-diluted samples were thereafter subjected to solid phase extraction (SPE) using vacuum aspiration and a silica based aminopropyl sorbent (GlycoWorks µElution Plate,Waters, Milford, MA). Wells containing 5 mg of sorbent were conditioned with water (200 µL), equilibrated with 85% (v/v) ACN (200 µL), and then loaded with the sample. Adsorbed samples were subsequently washed with

two, 600 µL volumes of a solution containing 1% formic acid in 90% acetonitrile (ACN). Lastly, enriched, labelled glycosylamines were eluted in three 30 µL elution volumes from the SPE sorbent using an eluent composed of 200 mM ammonium acetate (pH 7), 5% ACN. The obtained labelled N-glycosylamines were then diluted by addition of 100 µL DMF and 210 µL of ACN. Samples were stored at -80°C before analysis.

5.2.4. UPLC-FLR-MS analysis

Labelled *N*-glycans were analyzed via HILIC separations combined with fluorescence (FLR) and mass spectrometric (MS) detection using a UPLC-MS system equipped with a 2.1 x 150 mm, 1.7 µm, 130 Å column (ACQUITY UPLC BEH Amide, Waters Milford, MA) maintained at 55^{o}C. Gradient elution was performed using 50 mM ammonium formate pH 4.4 (A) and acetonitrile (B), with transition from 20:80 to 42:58 (A:B) over 39 mins, at a flow rate of 0.4 mL min^{-1}, with the exception of alpha1-acid glycoprotein where transition from 25:75 to 46:54 5A:B) over 35 mins was employed. Fluorescence was monitored at 265/425 nm (Ex/Em). MS data was acquired using a Single Quadrupole Detector 2, SQD2 (Waters Milford, MA) in ESI positive mode, with a capillary voltage of 3 kV, cone voltage of 30 V, source temperature of 150^{o}C, desolvation temperature of 350^{o}C and desolvation gas flow of 800 L h^{-1}. Data were acquired using Empower 3.1 software.

5.2.5. Data analysis

UPLC-FLR-MS data were processed and analyzed using Empower 3.1 software. FLR peak integration was automated and then checked and adjusted manually if necessary, to ensure consistency between samples. Peaks were assigned manually using MS spectra and relative retention time data. For relative quantitation, the FLR peak area for each *N*-glycan is expressed as a percentage of the total summed peak area for the identified glycan. Based on the mass of each glycan, the peak area was converted to mass percentage for comparison with FTIR spectra.

5.3. *FTIR measurements*

The FTIR measurements were performed with a Bruker Tensor 27 FTIR-spectrometer (Bruker Optics GmbH, Ettlingen, Germany) with the software Opus 6.5 (Bruker Optics GmbH, Ettlingen, Germany). The FTIR-spectrometer was equipped with a Mercury-Cadmium-Telluride detector, which was cooled down with liquid nitrogen. The spectra were recorded in the ATR mode by using a Golden GateTM ATR accessory (Specac, Orpington, United Kingdom) with an integrated total reflexion element composed of a single reflection diamond. The angle of incidence was 45 degrees.

For all glycoproteins, three independent samples were prepared. There was no sample digestion and only a buffer exchange step from raw material. To obtain triplicate measurements, the buffer-exchange step was repeated on three distinct days.

0.5 µL of sample was loaded on the diamond crystal of the ATR device of the FTIR spectrometer and quickly dried with a constant, gentle nitrogen flow: elimination of the water molecules prevents overlapping of the large water absorption peaks with the sample absorption spectrum. After each spectrum, the crystal was cleaned with water. A background was recorded with a clean crystal before the start of the measurements and before every new sample. FTIR spectra were recorded between 4000 and 600 cm^{-1} at a resolution of 2 cm^{-1}. Each spectrum was obtained by taking an average of 128 scans. The FTIR measurements were carried out at room temperature (~22°C). For each sample, six spectra were recorded. In total, for each protein, 18 FTIR spectra were recorded.

5.4. *FTIR data analysis*

5.4.1. Spectra preprocessing

All FTIR spectra were preprocessed as follows. The water vapor contribution was subtracted as described previously [17,18] with 1956-1935 cm^{-1} as reference peak. The spectra were then baseline-corrected. Straight lines were interpolated between spectrum absorbance at the following

wavenumbers: 3700, 3000, 2800, 1718, 1476, 1179, 965 and 865 cm^{-1}. They were then subtracted from the spectrum.

The sample thickness on the ATR crystal is not identical for all measurements. In order to compare samples according to the chemical composition, a normalization step is required. In this study, two normalization methods have been applied.

Firstly, normalization for equal area was applied between 1718 and 1476 cm^{-1}. This allows for comparison of samples considering the same quantity of proteins. Using this normalisation procedure, the spectral differences observed in the region of glycan absorption would be mainly due to differences in the weight ratio between glycans and proteins. Monitoring this ratio can therefore revealvariations in the global glycosylation level.

Secondly, normalization for equal area was applied between 1179 and 965 cm^{-1}. This allows for comparison of samples considering the same quantity of carbohydrates, and removes spectral variations due to the mass ratio between glycosylation and protein. Using this normalisation procedure, the spectral differences observed in the region of glycans are mainly due to differences in the glycan composition.

Outlier detection was performed after principal component analysis (PCA), the multivariate tool described below. A PCA was applied to all spectra of each antibody. A 85% confidence ellipse was built around the mean position of each glycoprotein in the score plot obtained in the PC1-PC2 space. For each antibody, the FTIR spectra that were outside the ellipse were considered as outliers. In total, 16 FTIR spectra were retained for further analyses for adalimumab, 17 for aflibercept, 15 for bevacizumab, 17 for cetuximab, 17 for infliximab, 16 for natalizumab, 17 for nivolumab, 17 for omalizumab, 15 for panitumumab, 17 for pembrolizumab, 18 for pertuzumab, 18 for ramucirumab, 18 for rituximab, 18 for trastuzumab and 17 for trastuzumab-emtasine.

5.4.2. Multivariate tools

In FTIR spectra, each wavenumber is a variable. With more than 200 wavenumbers associated with the absorption of glycosylation and with 16 to 18 spectra for each sample, the number of variables submitted to statistical analysis quickly becomes extremely large. Data are best handled after Principal Component Analysis (PCA), which is an unsupervised multivariate method that enables a reduction of variables by building linear combinations of wavenumbers that vary together [19]. Diagonalization of the covariance matrix of the data provides new variables, the so-called principal components (PC) holding all the correlated original variables on which original spectra are finally projected. The first principal component accounts for most of the variance present in the data set; the second is built with the residual variance and is uncorrelated to the first one. The subsequent components are constructed in the same way and account for the residual variance. In practice, almost all the variance of the original data can be explained with the four to six first PC, reducing the description of each spectrum to four to six numbers. Simultaneously, the weight of each PC in a spectrum characterizes a spectrum and allows an unsupervised classification of the spectra as such an observation does not suppose any *a priori* information on these groups [19]. In the analyses reported here, the collection of spectra was mean-centered (the mean was removed from the individual spectra). Whether a group is significantly different from the others was tested by multivariate analysis of variance (MANOVA) where each spectrum is identified by its projection on the first 4 principal components [20].

6. Results

Initially, the *N*-glycans of all glycoproteins (except fetuin) were characterized in detail as described in "Materials and methods" section. Table 1 summarizes the composition of major *N*-glycans or *N*-glycan types (quantified by relative peak area, % RPA) for each protein. GlycoWorks RapiFluor-MS *N*-glycan analysis was not performed on fetuin as it contains mainly *O*-glycans, which are not released by the PNGase F enzyme used in the protocol.

All *N*-glycans have a common core structure of five monosaccharides: a linear chain of two *N*-acetylglucosamines (GlcNAc) and a mannose, to which two further branching mannoses are attached. This elementary structure corresponds of all *N*-glycans is named M3 (see Figure 1). Additional mannoses can be added to form M4, M5, M6 … and other "high-mannose" glycans. Meanwhile, addition of fucose, GlcNAc, galactose (Gal) and *N*-acetylneuraminic acid (Neu5Ac; sialic acid) monosaccharides gives rise to a variety of "complex" *N*-glycan structures. The most abundant *N*-glycan in the therapeutic mAbs analysed here is the complex-type FA2. It possesses the M3 core structure but with a fucose attached to the first GlcNAc and extension of the branching mannoses with additional GlcNAc monosaccharides. Addition of β-linked galactose gives rise to FA2G1 and FA2G2, which can be terminated with sialic acids (including potentially immunogenic *N*-glycolylneuraminic acid, Neu5Gc) and/or α-linked galactose (also immunogenic).

Using the %RPA value of each *N*-glycan present in each sample (derived from HILIC-FLR data), along with the structure and the theoretical mass of each glycan, the total composition of monosaccharides in each sample has been calculated and is presented in Table 2.

It should be noted that aflibercept and cetuximab have the most distinguishable *N*-glycan profiles compared to other therapeutic proteins. Both samples possess the lowest percentages of FA2 *N*-glycan whilst cetuximab possesses the highest percentage of *N*-glycans containing alpha-linked galactose and aflibercept possesses the highest percentage of sialylated *N*-glycans. Similarly, cetuximab presents the highest overall galactose content and aflibercept the highest sialic acid content. Both samples have the lowest mannose and fucose contents.

Ribonuclease B and avidin have elevated proportions of high-mannose glycans, whilst alpha1-acid glycoprotein only contains sialylated glycans. This in accordance to the data described in the literature [10–13]. Fetuin has been characterized in several publications and is also known as a highly sialylated protein. [11,14,15]

In total 326 FTIR spectra were considered for further analysis. Figure 2 presents the mean spectra for each sample, scaled on the Amide I and II region. Large spectral variations can be observed between 1700 and 1500 cm^{-1}. Analysis of the shape of Amide I and II bands found between 1700 and 1500 cm^{-1} allows the determination of the secondary structure content, as described previously [21–23]. Distinct secondary structures are observed for proteins that are not mAbs. However, the focus in the present study is the spectral region between 1200 and 950 cm^{-1}, where large spectral variations can also be observed. These variations are mainly due to differences in the mass ratio between carbohydrate (i.e. glycosylation) and protein.

Figure 3 shows the mean spectra of each glycoprotein enlarged at the region of glycan absorption between 1200 and 950 cm^{-1}. Scaling has been performed between 1179 and 965 cm^{-1} to remove spectral variations due to different mass ratios of glycosylation and protein, allowing for comparison according to the glycan and monosaccharide band shape only. The FTIR spectra of all mAbs have a similar shape, whilst the spectra of aflibercept (yellow) and each of the 4 other glycoproteins have a unique shape and display significant variations to the spectra of mAbs.

Principal component analysis (PCA) is a tool frequently used to observe data clustering. Figure 4 shows the PCA score plot for all the data: mAbs and all the other proteins. FTIR spectra of pure sialic acid was also included in the analysis. Every point (star) in this plot is the projection of one spectrum in the space defined by the first two principal components (PC). The different proteins are identified by a unique colour (indicated in the right caption).

Two clusters can be observed and are circled in figure 4. The first one includes all mAbs and the second one contains all highly sialylated proteins (alpha1-acid glycoprotein, fetuin and aflibercept). Avidin and ribonuclease B are between the two clusters. These two proteins contain high-mannose

glycans but have a distinct *N*-glycans profiles as described in Table 1. The FTIR spectra of purified sialic acid are distinct from all other spectra, separated from all of the glycoproteins along principal component 1. The proteins with a high sialic acid content are also separated from the mAbs along PC1. However, sialic acid is not the only contribution to PC1; the 2 proteins with a majority of high-mannose glycans are also separated from mAbs along this axis.

In order to obtain further insight into the mAb spectra, Figure 5 presents the PCA score plot for the FTIR spectra of mAbs and aflibercept only. Figure 5A presents this data in the space defined by PC1 and PC2. It is notable that FTIR spectra of aflibercept and cetuximab now cluster separately from all the other FTIR spectra. As previously discussed, these two glycoproteins possess the most significant differences to the other mAbs in terms of *N*-glycan and monosaccharide composition. Figure 5B presents the same data in the space defined by PC3 and PC4, in which one protein (trastuzumab-emtasine) is clearly distinguished from all the others. This sample is the only antibody drug conjugate (ADC) analysed, of which the small molecule drug component may be responsible for the spectral variations.

Figure 6 shows the PCA score plot for the FTIR spectra of all therapeutic glycoproteins except aflibercept, cetuximab and trastuzumab-emtasine. Figure 6A presents the data in the space defined by PC1 and PC2 and Figure 6B in the space defined by PC3 and PC4. 95% confidence ellipses are also drawn around the mean position of each antibody indicated by a square for each group. In this case, differences between mAbs are less obvious but some mAbs are clearly distinct from each other. For example, bevacizumab and ramucirumab are clearly separated on Figure 6B. Score plots presented in figures 3 to 6 provide a quick overview of the data similarity. Yet, it must be stressed that PCA is unsupervised and does not optimize differences between groups. In particular, each plot presented compares the scores of only 2 PCs.

In order to test statistically the equality of the mean spectra considering their scores of the first 4 PCs, MANOVA analyses was carried out to investigate potential differences between the 12 therapeutic mAbs presented in Figure 6 (Table 3). This demonstrates that all the p-values are lower than 0.001. Statistically significant differences are therefore in evidence for every pair of mAbs.

7. Discussions and conclusions

Glycosylation is a critical quality attribute (CQA) of therapeutic glycoproteins. Regulatory agencies require detailed characterization and control of this parameter. However, the current methods involve multiple and lengthy sample preparation steps which can affect the robustness of the analyses. Orthogonal, direct and easier methods for glycosylation analysis are therefore desired. We propose use of FTIR spectroscopy to address this challenge, and aim to demonstrate that FTIR spectra of whole proteins can provide unique signatures sensitive to minor changes in the glycosylation profile.

In this study, we have recorded the FTIR spectra of 14 therapeutic mAbs, 1 therapeutic Fc-fusion protein and 4 other well-characterised glycoproteins. All samples were desalted prior to analysis to avoid any potential interference. Analysis was focused upon the spectral region between 1200 and 950 cm^{-1}, which is known to be largely due to glycan absorption. PCA performed using this specific spectral region demonstrates that FTIR spectral variations may be related to *N*-glycan and monosaccharide content. For example, fetuin, alpha1-acid glycoprotein and aflibercept are well-characterised as proteins with a high sialic acid content. Here, their FTIR spectra clearly present similarities with each other and differences with the other largely asialylated glycoproteins analysed. Additionally, the FTIR spectra of two proteins containing high-mannose glycans (ribonuclease B and avidin) show totally distinct characteristics.

We have then compared the FTIR spectra of the 14 mAbs. Interestingly, each sample has a unique FTIR profile, yet analyses using conventional *N*-glycan mapping techniques shows that they predominantly contain the same major *N*-glycans. This underlines that FTIR spectra can detect minor changes in the *N*-glycan and monosaccharide composition. Furthermore, specific spectral variations can also be detected among the FTIR spectra of mAbs. In particular, cetuximab which has the highest galactose content, displays a specific spectral signature. FTIR spectra of trastuzumab emtasine, the unique ADC in this study, also cluster separately, probably due to the emtasine absorption. Finally, by comparing FTIR spectra of all mAbs except cetuximab and trastuzumab-emtasine, we observed smaller but statistically significant differences. Each antibody, influenced by its glycosylation pattern, yields a specific fingerprint in the spectral region between 1200 and 950 cm^{-1}. The MANOVA

analysis (Table 3) indicates that the mean spectrum of each protein is unique, with no possible confusion ($p<1\%$) with another. This demonstrates that the FTIR spectrum successfully reports minor differences in the glycosylation profiles (Table 1).

One may ask whether other vibrational modes could contribute to the absorption band observed in the spectral region between 1200 and 950 cm^{-1}. Two non-glycosylated proteins (albumin and lysozyme) have also been analysed and compared with the glycoproteins analysed in this work (see supplemental figure). A slight absorption is observed in the spectral region between 1200 and 950 cm^{-1} (notably due to Amide III). However, the intensity of the absorption band is relatively low compared to that obtained in the same spectral range for glycoproteins. In addition, this contribution should be similar for all the proteins except for those with highly different structures. Aside from occasional exception, the contribution of protein to spectral absorption in the range 1200-950 cm^{-1} should not lead to errors in the interpretation of spectra in terms of *N*-glycan composition.

We have therefore demonstrated here that FTIR spectra of glycoproteins display spectral variations related to their *N*-glycan and monosaccharide compositions. FTIR spectra of glycoproteins provide a global fingerprint of all the glycans present in a sample, which is not only sensitive to large differences such as the presence of absence of some monosaccharides, as described previously [9], but also to smaller modifications as those occurring between different monoclonal antibodies used as therapeutics. FTIR spectroscopy, combined with statistical tools, can therefore be used to compare samples or batches in terms of glycosylation or monosaccharide profile. This method offers three key advantages.

Firstly, in comparison with all the existing method to analyse glycans and monosaccharides, it requires a very limited sample preparation. Analysis is performed on the whole protein, which represent a major advantage. Indeed, nowadays, all the existing methods to analyse glycans and monosaccharides involve several preparation steps: glycan release, labelling, separation, hydrolysis

for monosaccharide analysis, which can be complex and time-consuming, and introduce several potential sources of error. When conducting these assays, caution must be taken to ensure that glycans are effectively released, homogeneously labelled and recovered using appropriate procedures [3]. For example, it can be difficult to achieve complete *N*-glycan release; if not achieved then, the unreleased glycans are left undetermined. *N*-linked glycans are typically released by peptide-N-glycosidase F (PNGase F) which catalyses the cleavage between the reducing terminal GlcNAc and asparagine residue. This enzyme releases almost all *N*-glycans from proteins, with the exception of those bearing an α1-3 linked fucose residue attached to the reducing terminal GlcNAc residue. PNGase A can potentially be used as an alternative as this enzyme releases *N*-glycans containing the α1-3 linked fucose on the reducing terminal GlcNAC residue, yet shows lower efficiency in *N*-glycan release compared to PNGase F.*O*-glycanases are very specific to some particular carbohydrate moieties. *O*-linked glycans are therefore commonly released through reductive alkaline β-elimination, a process which is still not fully mastered. [1,3,6,24]. Glycan analysis should ideally involve procedures that only minimally alter the test samples and capture as much of the sample glycome as possible, as this is the case with a FTIR-based approach.

Secondly, the processing time is extremely short, especially in comparison with current LC-MS (liquid chromatography-mass spectrometry) or CE (capillary electrophoresis) procedures. The measurement of a FTIR spectrum takes a maximum of 5 minutes; the analysis in 96 or 384-well plates is already available and the use of microarrays of proteins is under development [25] , drastically increasing samples throughput. In addition, data analysis can be fully automated, dramatically reducing spectral interpretation time.

Finally, FTIR spectroscopy can be used as a Multi-Attribute Methodology (MAM) [26]. Analysis of other critical parameters for therapeutic proteins (such as the protein structure or protein concentration) can be performed simultaneously.

The main limitation of this approach is that FTIR spectroscopy is a global method. Information on specific residue or on specific glycosylation site cannot be extracted. Detailed characterization of the glycosylation will always be required for new drug application, involving several procedures such as

intact mass analysis, glycopeptide analysis and released glycan analysis. However, a FTIR-based approach presents obvious advantages for quality control, especially for in-process monitoring.

In conclusion, we propose three potential applications of a FTIR-based comparative approach:

1. For comparison of biosimilar candidates and the original molecule (innovator);
2. For batch-to-batch consistency checks for example during development, optimization and verification of the production process;
3. In-process controls (at-line or on-line requiring the development of some devices) to assess the reproducibility and the product quality during production processes.

In order to extend the range of applications of a FTIR-based approach, we will attempt to develop quantitative prediction tools to assist with determination of the major *N*-glycan and monosaccharide content using FTIR spectra.

8. References

[1] A. Planinc, J. Bones, B. Dejaegher, P. Van Antwerpen, C. Delporte, Glycan characterization of biopharmaceuticals: Updates and perspectives, Anal. Chim. Acta. 921 (2016) 13–27. doi:10.1016/j.aca.2016.03.049.

[2] R. Jefferis, Recombinant antibody therapeutics: the impact of glycosylation on mechanisms of action, Trends Pharmacol. Sci. 30 (2009) 356–362. doi:10.1016/j.tips.2009.04.007.

[3] L. Zhang, S. Luo, B. Zhang, Glycan analysis of therapeutic glycoproteins., MAbs. 8 (2016) 205–15. doi:10.1080/19420862.2015.1117719.

[4] P. Hossler, Protein Glycosylation Control in Mammalian Cell Culture: Past Precedents and Contemporary Prospects, in: Genomics Syst. Biol. Mamm. Cell Cult., Springer Berlin Heidelberg, Berlin, Heidelberg, 2011: pp. 187–219. doi:10.1007/10_2011_113.

[5] P. Hossler, S.F. Khattak, Z.J. Li, Optimal and consistent protein glycosylation in mammalian cell culture., Glycobiology. 19 (2009) 936–49. doi:10.1093/glycob/cwp079.

[6] L. Hajba, E. Csanky, A. Guttman, Liquid phase separation methods for N-glycosylation analysis of glycoproteins of biomedical and biopharmaceutical interest. A critical review, Anal. Chim. Acta. 943 (2016) 8–16. doi:10.1016/j.aca.2016.08.035.

[7] M. Hilliard, W.R. Alley, C.A. McManus, Y.Q. Yu, S. Hallinan, J. Gebler, et al., Glycan characterization of the NIST RM monoclonal antibody using a total analytical solution: From sample preparation to data analysis, MAbs. 9 (2017) 1349–1359. doi:10.1080/19420862.2017.1377381.

[8] K. Zheng, M. Yarmarkovich, C. Bantog, R. Bayer, T.W. Patapoff, Influence of glycosylation pattern on the molecular properties of monoclonal antibodies., MAbs. 6 (2014) 649–58. doi:10.4161/mabs.28588.

[9] M. Khajehpour, J.L. Dashnau, J.M. Vanderkooi, Infrared spectroscopy used to evaluate glycosylation of proteins., Anal. Biochem. 348 (2006) 40–8. doi:10.1016/j.ab.2005.10.009.

[10] M.J. Treuheit, C.E. Costellot, H.B. Halsall, Analysis of the five glycosylation sites of human x1-acid glycoprotein, 1992. https://www.ncbi.nlm.nih.gov/pmc/articles/PMC1131000/pdf/biochemj00138-0111.

[11] B.-S. Lee, S. Krishnanchettiar, S.S. Lateef, N.S. Lateef, S. Gupta, Characterization of oligosaccharide moieties of intact glycoproteins by microwave-assisted partial acid hydrolysis and mass spectrometry, Rapid Commun. Mass Spectrom. 19 (2005) 2553–2559. doi:10.1002/rcm.2096.

[12] H.J. An, T.R. Peavy, J.L. Hedrick, C.B. Lebrilla, Determination of N-Glycosylation Sites and Site Heterogeneity in Glycoproteins, Anal. Chem. 75 (2003) 5628–5637. doi:10.1021/ac034414x.

[13] R.C. Bruch, H.B. White, Compositional and structural heterogeneity of avidin glycopeptides., Biochemistry. 21 (1982) 5334–41. http://www.ncbi.nlm.nih.gov/pubmed/6816268.

[14] K.R. Anumula, Rapid Quantitative Determination of Sialic Acids in Glycoproteins by High-Performance Liquid Chromatography with a Sensitive Fluorescence Detection, Anal.

Biochem. 230 (1995) 24–30. doi:10.1006/ABIO.1995.1432.

[15] J. Baenziger, D. Fiete, Structure of the complex oligosaccharides of fetuin., J. Biol. Chem. 25 (1979) 789–795. http://www.jbc.org/content/254/3/789.

[16] M.A. Lauber, Y.-Q. Yu, D.W. Brousmiche, Z. Hua, S.M. Koza, P. Magnelli, et al., Rapid Preparation of Released *N* -Glycans for HILIC Analysis Using a Labeling Reagent that Facilitates Sensitive Fluorescence and ESI-MS Detection, Anal. Chem. 87 (2015) 5401–5409. doi:10.1021/acs.analchem.5b00758.

[17] E. Goormaghtigh, FTIR Data Processing and Analysis Tools, in: A. Barth, P.I. Haris (Eds.), Biol. Biomed. Infrared Spectrosc., IOS Press, 2009: pp. 104–128.

[18] E. Goormaghtigh, J. Ruysschaert, Subtraction of atmospheric water contribution in Fourier transform infrared spectroscopy of biological membranes and proteins, Spectrochim Acta. 50 (1994) 2137–2144.

[19] R.A. Johnson, D.W. Wichern, Principal Components, in: Appl. Multivar. Stat. Anal., 4th ed., Prentice Hall, Upper Saddle River, 1998: pp. 458–513.

[20] H.E. Johnson, A.J. Lloyd, L.A.J. Mur, A.R. Smith, D.R. Causton, The application of MANOVA to analyse Arabidopsis thaliana metabolomic data from factorially designed experiments, Metabolomics. 3 (2007) 517–530. doi:10.1007/s11306-007-0065-3.

[21] J.A. Hering, P.I. Haris, FTIR Spectroscopy for Analysis of Protein Secondary Structure, in: A. Barth, P.I. Haris (Eds.), Biol. Biomed. Infrared Spectrosc., IOS Press, 2009: pp. 129–167.

[22] A. Barth, C. Zscherp, What vibrations tell us about proteins., Q. Rev. Biophys. 35 (2002) 369–430. http://www.ncbi.nlm.nih.gov/pubmed/12621861.

[23] E. Goormaghtigh, V. Cabiaux, J.M. Ruysschaert, Determination of soluble and membrane protein structure by Fourier transform infrared spectroscopy. III. Secondary structures., Subcell Biochem. 23 (1994) 405–50. http://www.ncbi.nlm.nih.gov/pubmed/7855879.

[24] K.L. Ford, W. Zeng, J.L. Heazlewood, A. Bacic, Characterization of protein N-glycosylation by tandem mass spectrometry using complementary fragmentation techniques., Front. Plant Sci. 6 (2015) 674. doi:10.3389/fpls.2015.00674.

[25] J. De Meutter, J. Vandenameele, A. Matagne, E. Goormaghtigh, Infrared imaging of high density protein arrays., Analyst. 142 (2017) 1371–1380. doi:10.1039/c6an02048h.

[26] P.C. Groß, M. Zeppezauer, Infrared spectroscopy for biopharmaceutical protein analysis, J. Pharm. Biomed. Anal. 53 (2010) 29–36. doi:10.1016/J.JPBA.2010.03.009.

9. Acknowledgement

This research has been supported by the "Service Public de Wallonie – DGO6" (Walinnov 2017/2, convention # 1710032).

E.G. is Director of Research with the ''National Fund for Scientific Research'' (Belgium), A.D. is Research Fellow supported by the "Service Public de Wallonie – DGO6". We are grateful to Serge Van Praet and Florence Rappez (Pharmacy, CHU Saint-Pierre, Brussels, Belgium) for providing us all the therapeutic proteins.

10. Table captions:

Table 1: Mass percentages (calculated based on relative peak areas - %RPA) of major *N*-glycans or *N*-glycan types for each glycoprotein. This percentage has been obtained based on the percentages (relative peak area) derived from UPLC-FLR-MS analysis of the *N*-glycans released, labelled and purified using the GlycoWorks RapiFluor-MS *N*-glycan kit from Waters. MS data was used to identify *N*-glycans and FLR data was used for the relative quantification.

Table 2: Overall mass percentages of the 5 monosaccharides that are present in protein glycosylation. These values were calculated using %RPA and the monosaccharide composition of each *N*-glycan.

Table 3: p-values calculated by Multivariate Analysis of Variance (MANOVA) of the first 4 principal components between each pair of monoclonal antibodies. Principal components are computed between 1179 and 965 cm^{-1}. The scores of the first 4 components of all the 15 to 18 spectra for each antibody were submitted to MANOVA.

11. Figure captions:

Figure 1: Structures of several typical *N*-glycans.

Figure 2: Mean infrared spectra of the preprocessed spectra of each glycoprotein between 1800 and 850 cm^{-1}. Each protein is depicted in a unique colour, as annotated. At least 15 spectra per antibody and 6 spectra for the other proteins were used for computing the mean spectra. Spectra were preprocessed as described in Materials and Methods and have been normalized between 1718 and 1476 cm^{-1}. Spectra have been offset for better readability.

Figure 3: Mean infrared spectra of the preprocessed spectra of each glycoprotein between 1200 and 950 cm^{-1}. Each protein is depicted in a unique colour, as annotated. At least 15 spectra per protein were used for computing the mean spectra. Spectra were preprocessed as described in the Materials and Methods and have been normalized between 1179 and 965 cm^{-1}.

Figure 4: PCA score plot of the 326 individual preprocessed FTIR spectra in the PC1-PC2 performed on the 1179-965 cm^{-1} spectral region. Each star represents one spectrum. For the sake of clarity, a colour is associated with each sample. Percentages on the axis labels indicate the variance described by PC1 (88.6%) and PC2 (6.49%). The preprocessing of the spectra is described in Materials and Methods. Spectra have been normalized between 1179 and 965 cm^{-1}. A mean centering was applied on this set of data prior to PCA.

Figure 5: PCA score plot of the 253 individual preprocessed FTIR spectra in the PC1-PC2 space (A) and in the PC3-PC4 space (B) performed on the 1179-965 cm^{-1} spectral region. Each star represents one spectrum. For the sake of clarity, a colour is associated with each sample. Percentages on the axis labels indicate the variance described by PC1 (85.9%), PC2 (8.15%), PC3 (3.7%) and PC4 (1.14%). The preprocessing of the spectra is described in Materials and Methods. Spectra have been normalized between 1179 and 965 cm^{-1}. A mean centering was applied on this set of data.

Figure 6: PCA score plot of the 202 individual preprocessed FTIR spectra in the PC1-PC2 space (A) and in the PC3-PC4 space (B) performed on the 1179-965 cm^{-1} spectral region. Each star stands for one spectrum. For the sake of clarity, a colour is associated with each sample. Percentages on the axis labels indicate the variance described by PC1 (55.7%), PC2 (28.2%), PC3 (7.49%) and PC4 (3.93%). The square is the position of the mean. 95% confidence ellipses around the mean position of each cluster were computed. The preprocessing of the spectra is described in Materials and Methods. Spectra have been normalized between 1179 and 965 cm^{-1}. A mean centering was applied on this set of data.

Supplemental figure: Mean infrared spectra of the preprocessed spectra of each glycoprotein and two not glycosylated proteins (albumin and lysozyme) between 1200 and 950 cm^{-1}. Proteins are indicated by the colour described in the caption on the right of the figure. Spectra were preprocessed as described in the Materials and Methods and have been normalized between 1718 and 1476 cm^{-1}. This normalization allows a comparison of samples with a similar quantity of proteins and evidences variations in the mass ratio between glycans and proteins.

Table 1

	FA2	FA2G1	FA2G2	M5	High mannose (M6, M7, M8, M9)
Adalimumab	68.83	15.93	1.16	4.88	3.77
Aflibercept	6.13	9.78	4.59	1.92	0.00
Bevacizumab	79.92	11.49	1.41	0.51	0.00
Cetuximab	18.39	18.27	3.58	3.84	0.33
Infliximab	44.30	27.67	4.09	2.26	0.00
Natalizumab	52.89	30.52	5.20	0.81	0.00
Nivolumab	56.70	30.26	5.76	0.64	0.79
Omalizumab	61.78	20.21	1.67	4.45	0.69
Panitumumab	35.58	39.35	8.18	4.91	3.75
Pembrolizumab	67.84	19.70	2.54	0.85	0.59
Pertuzumab	83.33	8.71	0.72	0.76	0.25
Ramucirumab	20.18	43.57	14.24	0.43	0.00
Rituximab	63.20	23.67	4.68	1.04	0.58
Trastuzumab	57.84	28.39	3.50	1.12	0.05
Trastuzumab emtasine	62.90	23.89	2.27	1.19	0.06
Ribonuclease B	0.00	0.00	0.43	23.66	65.92
Avidin	0.00	0.00	0.00	7.23	20.29
Alpha1-acid glycoprotein	0.00	0.00	0.00	0.00	0.00

Table 2

Mass ratio %	Mannose	N-acetylglucosamine	Galactose	Fucose	Sialic Acid
Adalimumab	36.35	52.68	1.95	9.02	0.00
Aflibercept	27.03	42.18	**13.51**	4.47	**12.81**
Bevacizumab	33.43	54.99	1.62	9.73	0.23
Cetuximab	28.89	44.13	**16.19**	7.84	**2.95**
Infliximab	34.46	50.86	5.12	8.59	0.96
Natalizumab	31.92	52.49	5.42	9.53	0.64
Nivolumab	32.55	53.16	4.57	9.30	0.43
Omalizumab	35.01	53.17	2.68	8.93	0.21
Panitumumab	35.41	50.14	6.10	8.30	0.05
Pembrolizumab	33.25	54.19	2.88	9.23	0.45
Pertuzumab	33.93	55.27	1.06	9.74	0.01
Ramucirumab	29.89	48.83	**11.22**	8.81	1.25
Rituximab	33.10	53.50	3.62	9.40	0.37
Trastuzumab	33.02	53.71	3.87	9.18	0.23
Trastuzumab emtasine	33.33	53.98	3.17	9.30	0.22
Ribonuclease B	67.64	30.22	1.55	0.33	0.26
Avidin	42.19	45.15	12.15	0.00	0.51
Alpha1-acid glycoprotein	16.24	35.61	17.59	0.86	29.70

Table 3

P-values	Adalimumab	Bevacizumab	Infliximab	Natalizumab	Nivolumab	Omalizumab
Adalimumab	1.00E+00					
Bevacizumab	< E-20	1.00E+00				
Infliximab	1.07E-14	1.66E-13	1.00E+00			
Natalizumab	9.79E-14	1.60E-11	4.65E-03	1.00E+00		
Nivolumab	1.91E-13	< E-20	1.62E-11	8.70E-12	1.00E+00	
Omalizumab	4.89E-13	1.77E-05	4.25E-08	7.40E-04	1.03E-12	1.00E+00
Panitummab	3.96E-11	1.11E-16	2.22E-16	< E-20	< E-20	1.89E-15
Pembrolizumab	1.67E-15	1.31E-14	2.52E-03	1.99E-07	2.39E-12	2.24E-07
Pertuzumab	< E-20	6.24E-11	3.95E-08	7.14E-09	1.67E-15	1.90E-04
Ramucirumab	1.73E-13	< E-20	2.44E-15	4.77E-15	2.81E-04	9.55E-15
Rituximab	< E-20	5.39E-13	4.53E-06	3.85E-08	4.26E-13	1.83E-09
Trastuzumab	2.48E-11	< E-20	4.87E-09	1.52E-07	3.48E-10	1.15E-09

Figure 1

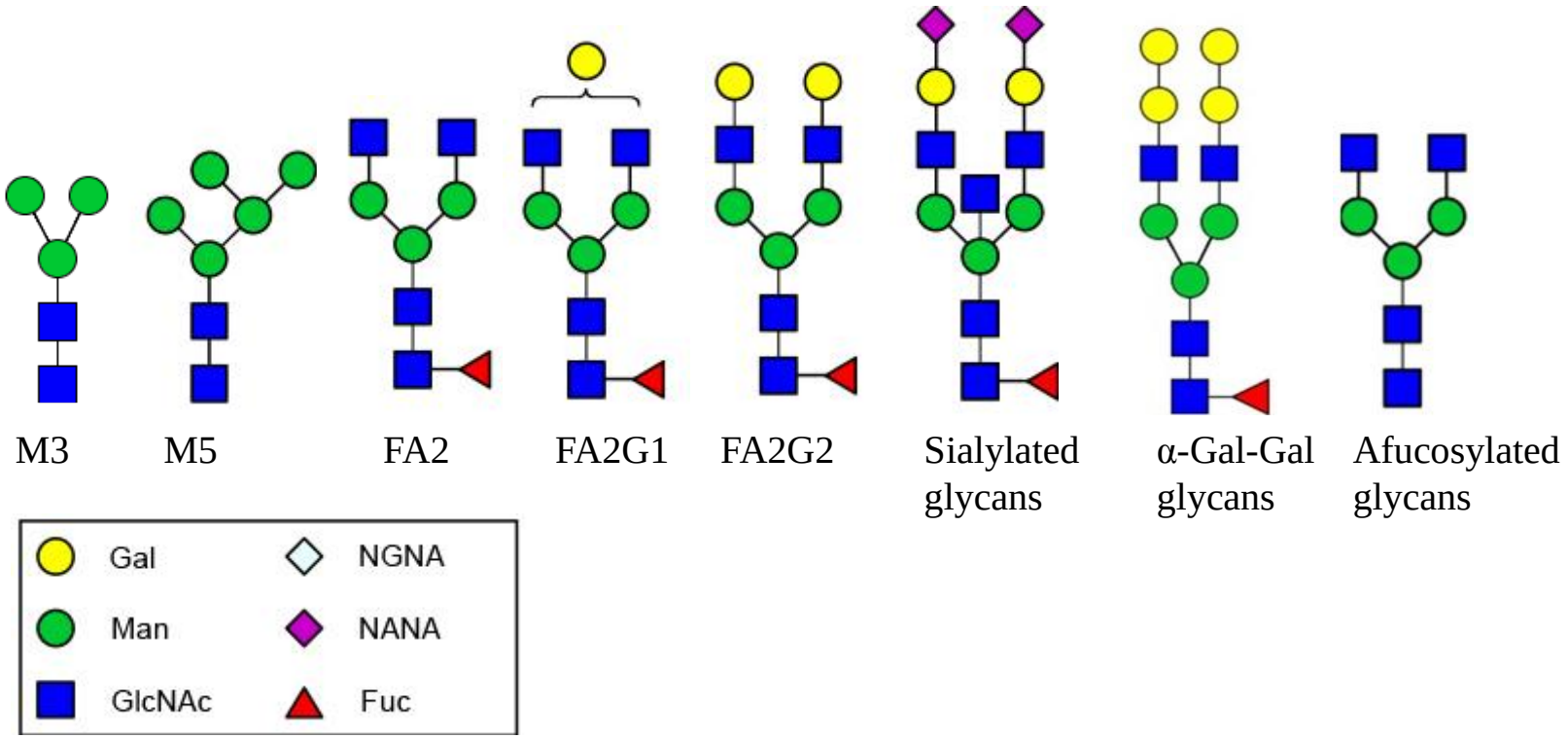
M3
M5
FA2
FA2G1
FA2G2
Sialylated glycans
α-Gal-Gal glycans
Afucosylated glycans
Gal
Man
GlcNAc
NGNA
NANA
Fuc

Figure 2

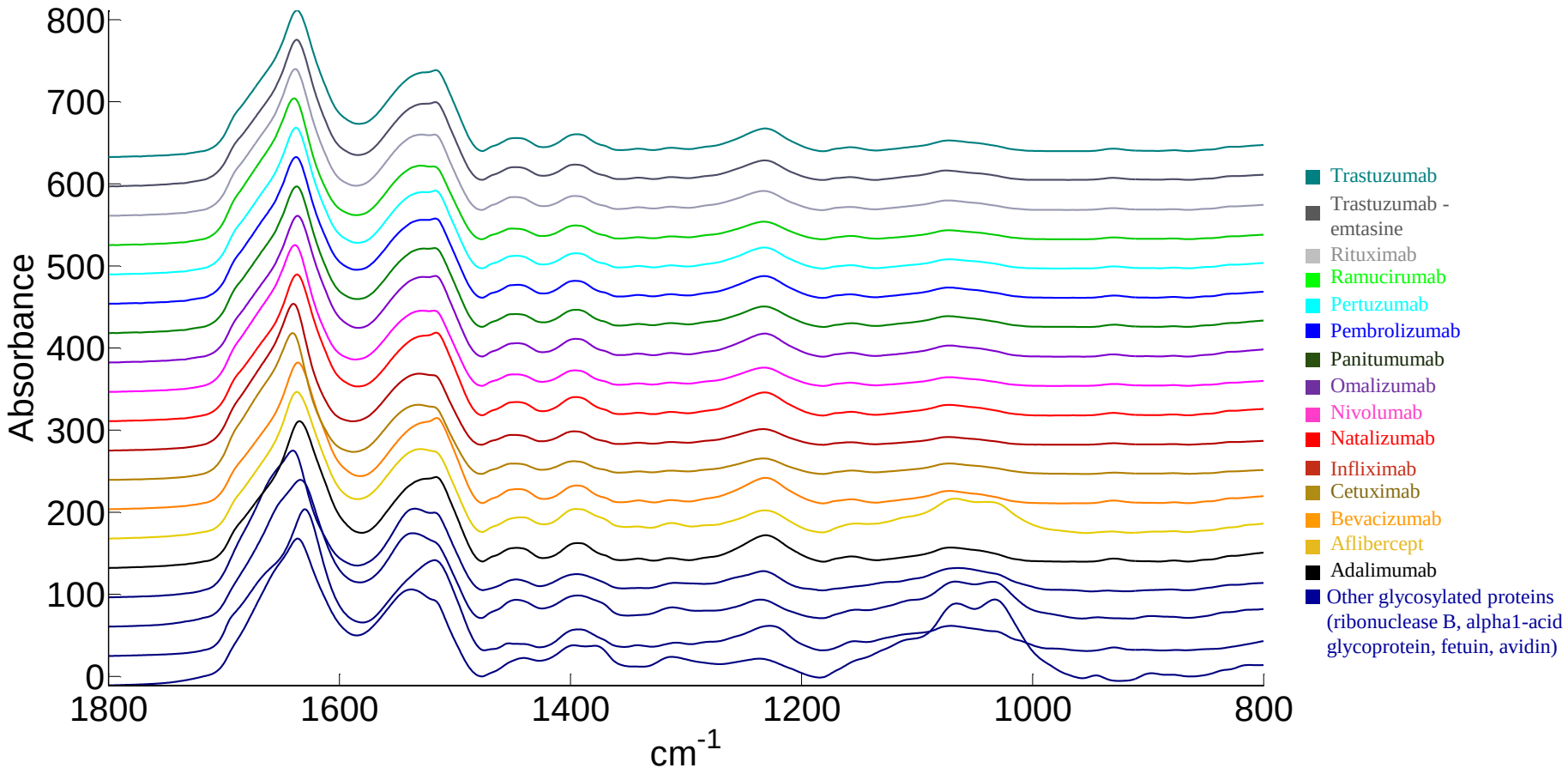
800
700
600
500
400
300
200
100
0
Absorbance
1800
1600
1400
1200
1000
800
cm-1
Trastuzumab
Trastuzumab - emtasine
Rituximab
Ramucirumab
Pertuzumab
Pembrolizumab
Panitumumab
Omalizumab
Nivolumab
Natalizumab
Infliximab
Cetuximab
Bevacizumab
Aflibercept
Adalimumab
Other glycosylated proteins (ribonuclease B, alpha1-acid glycoprotein, fetuin, avidin)

Figure 3

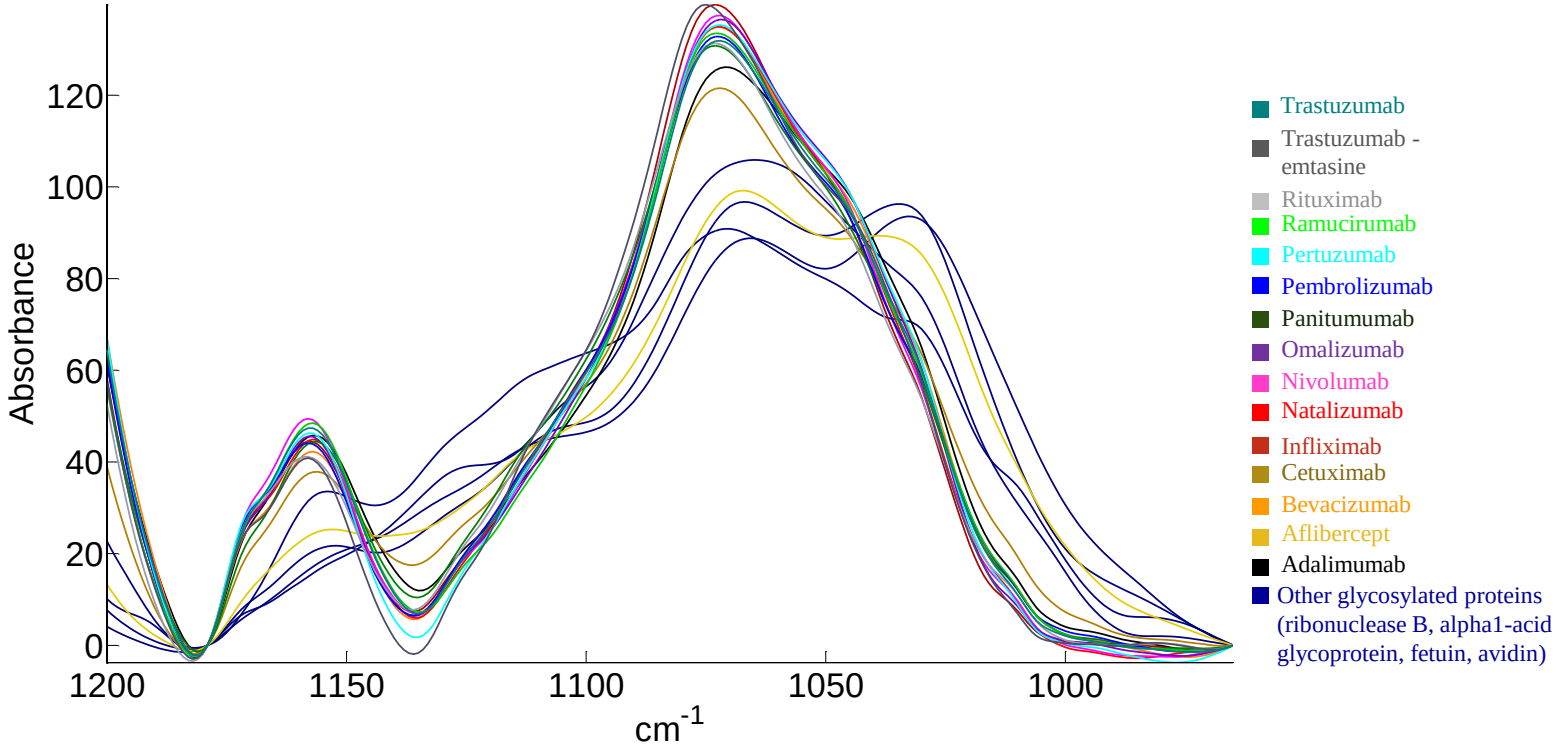
Absorbance
120
100
80
60
40
20
0
1200
1150
1100
1050
1000
cm-1
Trastuzumab
Trastuzumab - emtasine
Rituximab
Ramucirumab
Pertuzumab
Pembrolizumab
Panitumumab
Omalizumab
Nivolumab
Natalizumab
Infliximab
Cetuximab
Bevacizumab
Aflibercept
Adalimumab
Other glycosylated proteins (ribonuclease B, alpha1-acid glycoprotein, fetuin, avidin)

Figure 4

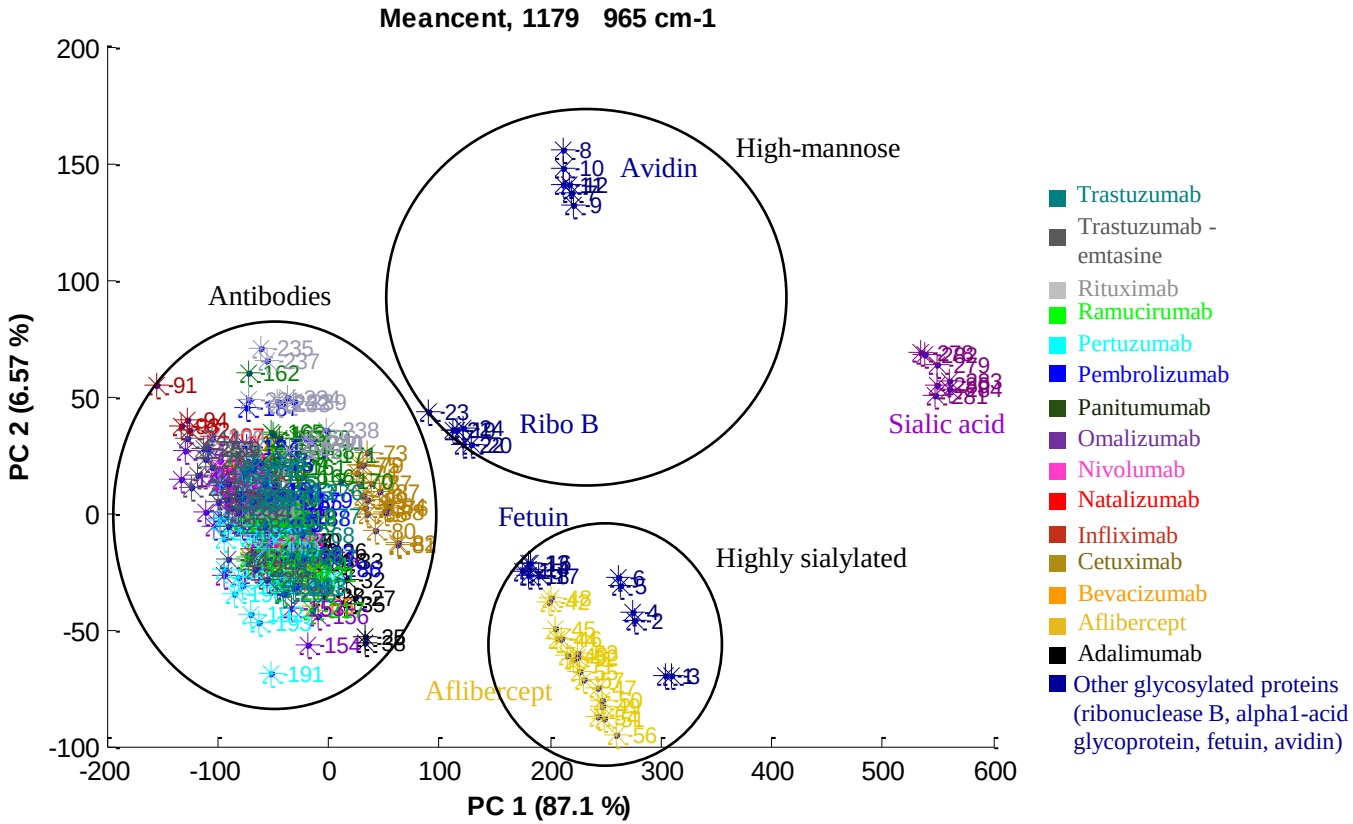
Meancent, 1179 965 cm-1
PC 2 (6.57 %)
PC 1 (87.1 %)
High-mannose
Avidin
Antibodies
Ribo B
Sialic acid
Fetuin
Highly sialylated
Aflibercept
Trastuzumab
Trastuzumab - emtasine
Rituximab
Ramucirumab
Pertuzumab
Pembrolizumab
Panitumumab
Omalizumab
Nivolumab
Natalizumab
Infliximab
Cetuximab
Bevacizumab
Aflibercept
Adalimumab
Other glycosylated proteins (ribonuclease B, alpha1-acid glycoprotein, fetuin, avidin)

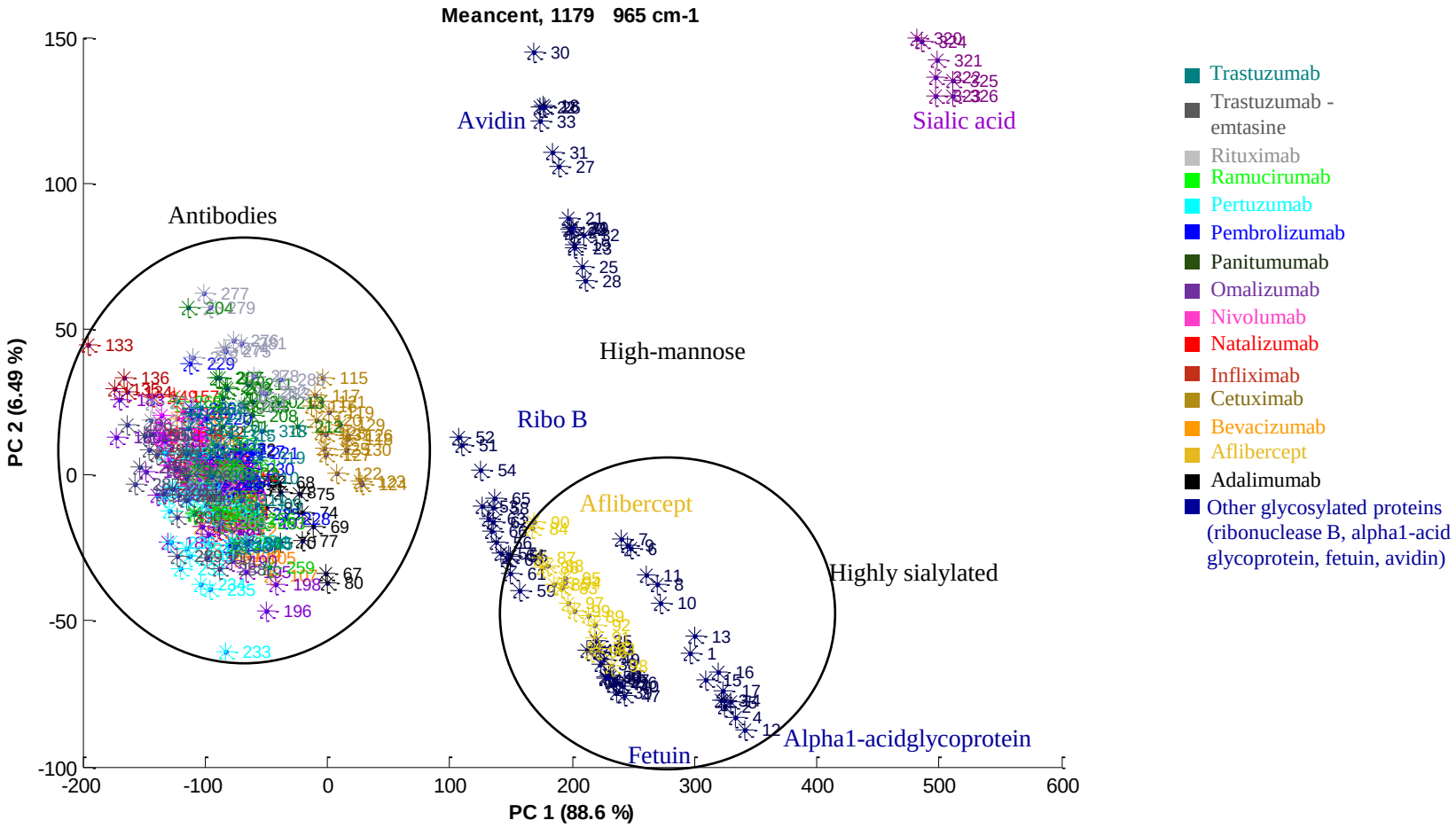
Meancent, 1179 965 cm-1
PC 2 (6.49 %)
PC 1 (88.6 %)
Antibodies
Avidin
Sialic acid
High-mannose
Ribo B
Aflibercept
Highly sialylated
Fetuin
Alpha1-acidglycoprotein
Trastuzumab
Trastuzumab - emtasine
Rituximab
Ramucirumab
Pertuzumab
Pembrolizumab
Panitumumab
Omalizumab
Nivolumab
Natalizumab
Infliximab
Cetuximab
Bevacizumab
Aflibercept
Adalimumab
Other glycosylated proteins (ribonuclease B, alpha1-acid glycoprotein, fetuin, avidin)

Figure 5

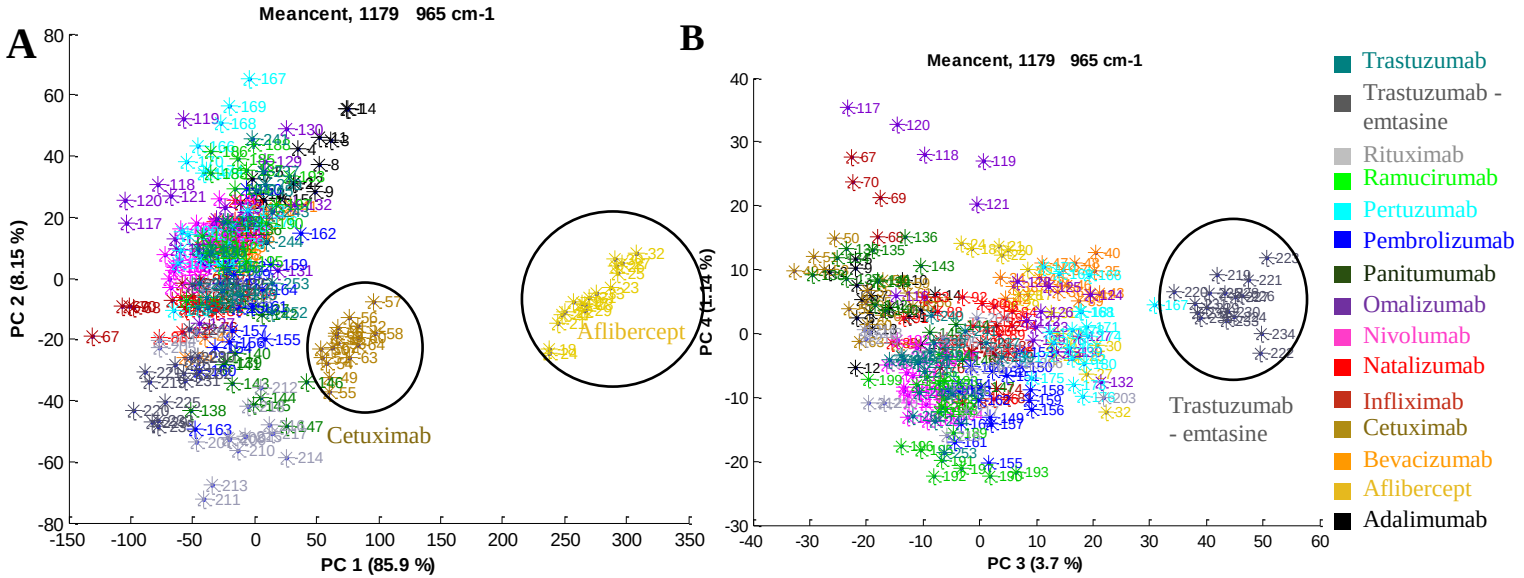
A
Meancent, 1179 965 cm-1
PC 2 (8.15 %)
PC 1 (85.9 %)
Cetuximab
Aflibercept
B
Meancent, 1179 965 cm-1
PC 4 (1.14 %)
PC 3 (3.7 %)
Trastuzumab - emtasine
Trastuzumab
Trastuzumab - emtasine
Rituximab
Ramucirumab
Pertuzumab
Pembrolizumab
Panitumumab
Omalizumab
Nivolumab
Natalizumab
Infliximab
Cetuximab
Bevacizumab
Aflibercept
Adalimumab

Figure 6

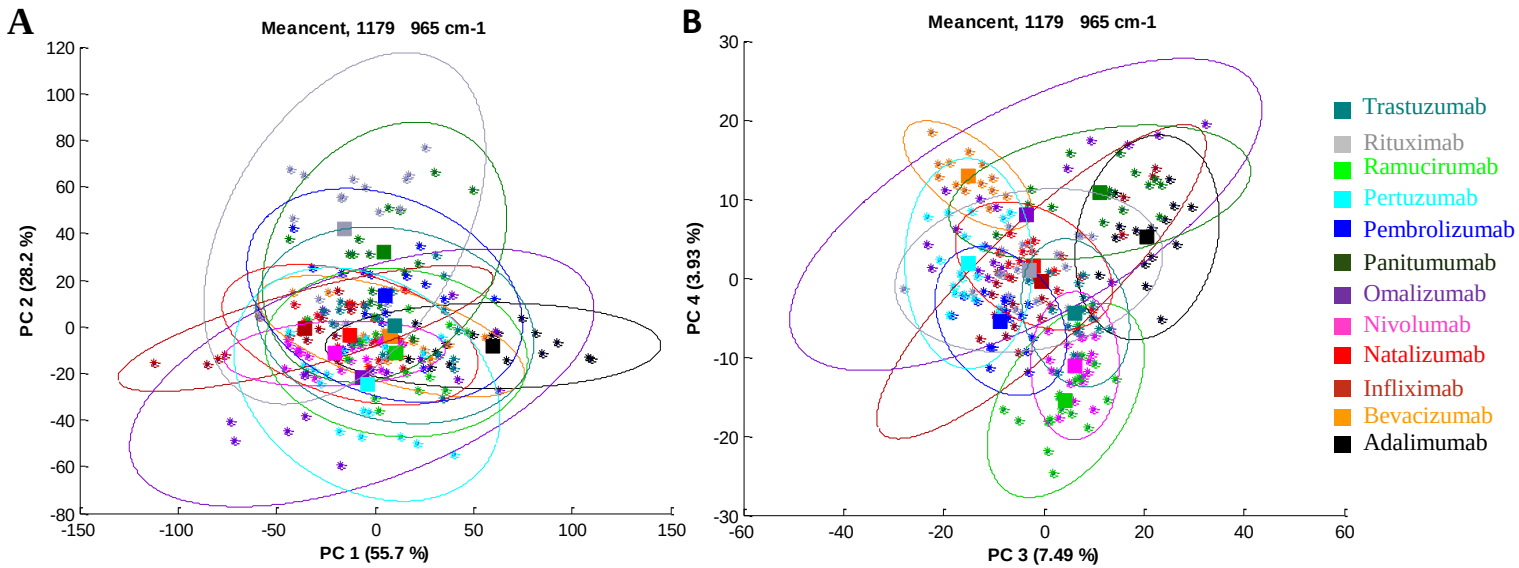
A
Meancent, 1179 965 cm-1
PC 2 (28.2 %)
PC 1 (55.7 %)
B
Meancent, 1179 965 cm-1
PC 4 (3.93 %)
PC 3 (7.49 %)
Trastuzumab
Rituximab
Ramucirumab
Pertuzumab
Pembrolizumab
Panitumumab
Omalizumab
Nivolumab
Natalizumab
Infliximab
Bevacizumab
Adalimumab